CHINESE OPTICS LETTERS

Vol. 19, No. 8 | August 2021

Proposal for experimentally observing expectant ball lightning

Silin Guo (郭丝霖)[1], Zhongpeng Li (李中鹏)[1,2], Chuliang Zhou (周楚亮)[1,2], and Ye Tian (田 野)[1,2*]

[1] State Key Laboratory of High Field Laser Physics and CAS Center for Excellence in Ultra-Intense Laser Science, Shanghai Institute of Optics and Fine Mechanics, Chinese Academy of Sciences, Shanghai 201800, China

[2] Center of Materials Science and Optoelectronics Engineering, University of Chinese Academy of Sciences, Beijing 100049, China

*Corresponding author: tianye@siom.ac.cn

Received November 11, 2020 | Accepted February 2, 2021 | Posted Online April 22, 2021

Ball lightning is widely concerning because it is hard to detect, predict, and reproduce. The dependences of electromagnetic (EM) solitons, which are considered expectant ball lightning, forming at the wavelength of the incident light are investigated with two-dimensional particle-in-cell simulations. It shows that both the long wavelength microwave and the short wavelength laser are not suitable for producing the observed ball-lightning-like EM solitons. A strong field terahertz wave is proposed to inject and generate EM solitons. This paper can provide some references for researchers studying ball lightning.

Keywords: expectant ball lightning; electromagnetic solitons; terahertz.
DOI: 10.3788/COL202119.083201

1. Introduction

Thunderstorms, lightning, and various electrical phenomena can be seen everywhere in our life. The exploration of these electrical phenomena has never stopped, and some phenomena, like the generation, propagation, and adhesion processes of lightning, and the compact in-cloud discharge phenomenon can be explained by the generation, transmission, and interaction of high-energy particles in the atmosphere with air atoms forming low-energy electrons and ions[1]. Femtosecond laser filamentation in air can be used to study a series of physical phenomena such as discharge or spectroscopy[2,3]. Among many electrical phenomena, ball lightning, a peculiar physical phenomenon that is rarely observed, has attracted much attention[4,5]. Ball lightning is a symbiotic structure of a spherical membrane of compressed air and conventional white light circulating in the membrane in all possible directions[6,7]. Many researchers have published theoretical models of ball lightning, such as models using assumptions about oscillation of electrons and ions[8,9], models involving resonant electromagnetic (EM) structures[10], and the magnetic-knot model[11,12], in an attempt to explain its formation mechanism, light emission, lifetime, and some other unusual characteristics. Subsequently, based on these theories, numerous experimental attempts to generate ball lightning in the laboratory have sprung up[13–15]. Among these theoretical models of ball lightning, the one that interests us most is Wu's extension[10] of the Dawson–Jones model[16], that is, before the final step of lightning striking the ground, a collimated electron bunch containing up to 10^{14} electrons could emerge. A concentrated relativistic electron bunch like that would emit an intense EM pulse when it strikes the ground or other media, which have greatly different dielectric properties from air. When EM pulses encounter plasma, a bubble where a region of low-density plasma surrounded by higher-density plasma could be formed. There are many characteristics between EM solitons and ball lightning. First, the size of the reported ball lightning is consistent with that of the EM solitons in the micron-scale laser plasma simulation. EM solitons are plasma bubbles containing half-cycle standing wave modes, whose wavelengths can reach several tens of centimeters in half a period when it comes to microwaves, which is similar to ball lightning. Besides, hundreds of joules of microwaves could keep a bubble's plasma shell alive for several seconds, which imitates the formation of post-solitons[17] and is similar to the typical ball lightning lifetime of 1–5 s[18]. In addition, ball lightning is spherical in shape, which is similar to the EM soliton created in laser plasma experiments. Thus, the EM solitons in the laser–plasma interaction can be considered as an expectant ball lightning object. The phenomenon of self-sustaining standing waves similar to solitons can be predicted under numerical simulation of appropriate density plasma and amplitude EM pulses[10], which provides guidance for our experimentally generated expectant ball lightning. In this article, the expectant ball lightning EM solitons generation distribution in intensity and density domain at different wavelengths of the incident EM wave are simulated with two-dimensional particle-in-cell (PIC) simulations. Our simulation

shows that the phenomenon of expectant ball lightning EM solitons can be observed regardless of the incident wavelength. The energy of the pulse from Wu's estimation is concentrated in the microwave region; however, the largest microwave-pulse facility currently[19] still cannot reach the energy to generate an expectant ball lightning EM soliton. This requires the medium to be preionized in order to produce sufficient density plasma during the experiment, which is too demanding for the experimental conditions. Meanwhile, using short wavelength EM waves such as X rays is also difficult to observe experimentally, according to our simulation results. Therefore, we make a proposal to generate expectant ball lightning EM solitons ("solitons" for short in the following article) through the interaction of strong field terahertz (THz) waves with gas plasma. Our proposal makes it possible to generate simulated ball lightning under laboratory conditions, thus laying the foundation for its systematic study.

2. Simulations

Simulations were carried out with the code extendable PIC open collaboration (EPOCH, a plasma physics simulation code that uses the PIC method) with relativistic electrons and immobile ions since the generation of post-solitons was not considered. The transverse width and the longitudinal duration of the incident laser pulse both had a Gaussian envelope with full width at half-maximum (FWHM) sizes of 2λ and $2T$, respectively. The cell size was $0.02 \times 0.02\lambda^2$, where λ was the wavelength of the incident laser, and each cell contained 10 ions and 10 electrons. The density and laser intensity were normalized over n_c and $a_0 = eE/(m_e\omega c)$, where c, m_e, and e were the speed of light in vacuum, the mass, and the charge of the electron, respectively. Moreover, T and ω were the period and circular frequency of the incident laser. Generally speaking, a steeper vacuum–plasma interface will result in weaker solitons. In our simulations, however, a steep vacuum–plasma interface was set in order to reduce the influence of interface gradient. The stability of EM solitons could be observed in simulations when moderate parameters for laser and plasmas were selected. Figure 1 portrays the temporal evolution of the electric field in the center of the EM soliton and the magnetic field in the soliton off center, owing to the magnetic field being annular around the center, when a linearly s-polarized laser propagates through the plasma with the density $n_e = 0.5n_c$ from 30 T to 50 T. The component of the magnetic field in the direction of laser propagation is shown in Fig. 1(b) to facilitate the extraction of the data. The normalized value of the laser was $a = 1$, corresponding to the electric field intensity of 1.07×10^{12} V/m, while the wavelength was 3 μm. The vibration of the electric field precedes that of the magnetic field for a quarter of the oscillation period because, when the electric field reaches its maximum, the size of the electron cavity is maximized, and the corresponding current is zero in the solitons[20]. In addition, the frequency of the component of the electric field was about 0.55ω [Fig. 1(c)], which was a little bit smaller than the localized Langmuir frequency around the soliton. The electron density profile along the direction of the laser propagation is depicted in Fig. 1(d), where a valley represents the soliton. It is noticeable that the density of the localized electrons is a little higher than the background density and exceeds $0.6n_c$, which means that the Langmuir frequency is over 0.77ω. Hence, EM waves can be captured stably and efficiently.

Figure 2 schematically displays the spatial distribution of electrons with two different initial number densities at different moments of time. The soliton in Fig. 2(a) with an initial density of $1.3n_c$ is closer to the vacuum–plasma interface than that in Fig. 2(b), where the initial density is $0.25n_c$. When the initial density is just slightly higher than the critical density, the laser can still penetrate into the plasma. The leading edge of the laser

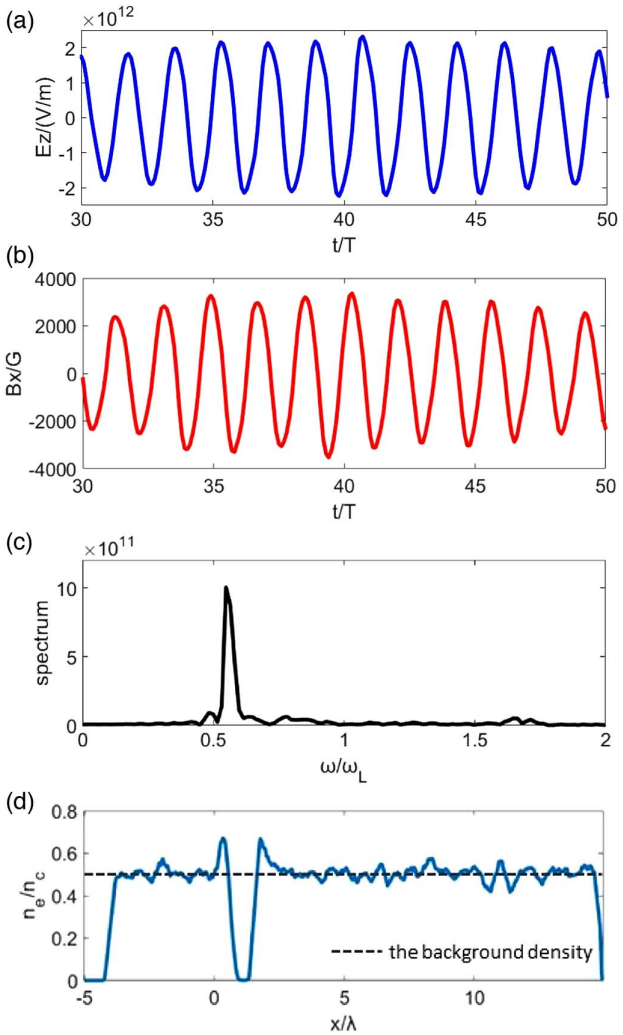

Fig. 1. Temporal evolution of (a) electric field and (b) magnetic field. The electric and magnetic fields are oscillated periodically, and the magnetic field lags quarter of an oscillation period behind the electric field. Panel (c) shows the Fourier transformation of the electric field from 0 T to 60 T, i.e., the spectrum of the soliton. There is a monoenergetic peak in frequency domain referring to the soliton frequency. Panel (d) is the lineout of longitudinal density of the electrons. The vacuum–plasma interface is at -4λ, and the density valley around 1λ is where the soliton position is. The localized density on either side of the valley is slightly higher than the background density.

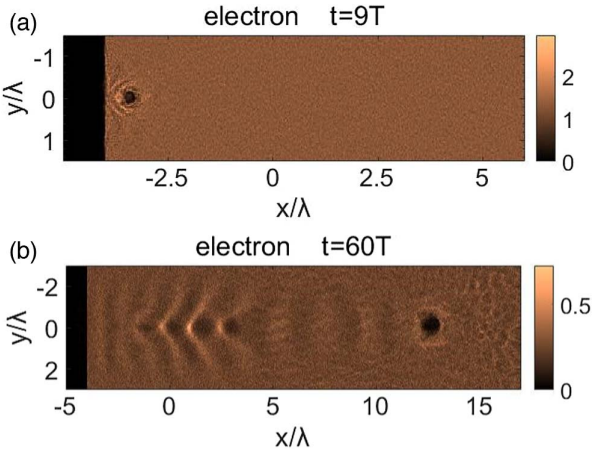

Fig. 2. Distributions of electrons in the cases of (a) density close to upper limit and (b) lower limit of soliton generation for $a = 1$. The units of density, time, and length are critical plasma density, laser period, and wavelength, respectively. The soliton in panel (a) stays stationary near the interface, while the soliton in panel (b) stays at some distance away from the interface. The periodic density hump between vacuum–plasma interface and the soliton in panel (b) is the trail of the laser wakefield. It is obvious that the size of the two solitons is different.

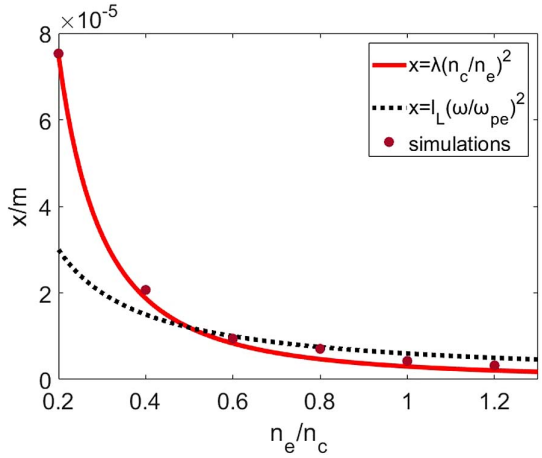

Fig. 3. Relationship between plasma density and the distance from the position of the solitons to the vacuum–plasma interface is drawn. For a fixed normalized value $a = 1$, the distance from the interface of the solitons decreases with an increase in the number density of electrons. The red solid curve is more consistent with the simulation results than the gray dotted curve.

compresses the electron surface into a concave, which in turn reflects the laser frontier. Because of the immobile ions, the electrons oscillate near the interface due to electrostatic forces, and the speed of the electrons is slower than the speed of light in vacuum. Consequently, the electrons will follow the laser frontier. Once the process is repeated and accumulated to a certain extent, subsequent EM waves will be captured by the plasma. In this case, the frequency of the solitons is not much lower than that of the laser due to less photon energy loss. When the initial plasma is underdense, the laser can propagate through the plasma and generate a wakefield behind the laser due to the ponderomotive force. The wakefield continuously gains energy from the laser, resulting in the downshift of the laser frequency. Once the frequency of the EM waves is less than the localized Langmuir frequency, the EM soliton is generated, as shown in Fig. 2(b), namely, the depth of penetration determined by the redshift rate, which depends on plasma density, laser pulse duration, and intensity[21]. The trail of the wakefield is distinctly shown in the figure, indicating that solitons generated in this case are related to the wakefields. Moreover, the plasma cavity in Fig. 2(a) is apparently bigger than that in Fig. 2(b), because the size of the solitons is of the order of $d_e = c/\omega_{pe}$[22], where d_e is the electron skin depth, and ω_{pe} is the Langmuir frequency. The distribution of electrons when the laser wavelength was different had also been investigated, and we found that the size of the plasma cavities has almost no difference to the case above.

Note that the position of the solitons is related to the density of plasmas, and thus simulations of the relationship between the two were performed. From Fig. 3, we can infer that solitons tend to be generated close to the interface as the density increases. It is also found that the greater the density is, the smaller the position change is. Researches on the position of solitons related to the plasma density had been mentioned by numerous authors[22–25]. In all these works, a unanimous assumption of the laser pulse depletion had been adopted with the form of $l_{\text{depth}} = l_L(\omega/\omega_{pe})^2$, where l_L is the duration of the incident laser pulse. However, the results provided from this formula could lead to obvious error in simulations because Raman scattering was not concerned. We discovered from the simulations that the dependence of the solitons' position on plasma density can be explained as $l_s = \lambda(n_c/n_e)^2$, where l_s is the distance from the position of the solitons to the vacuum–plasma interface. The curve drawn by this formula in Fig. 3 shows that the formula fits the simulations very well, especially when the relative plasma density is lower than 0.5. Combined with Fig. 2, the generation of solitons far away from the interface is inseparable from the wakefield. The laser has to propagate for a long distance to loose enough energy so that the frequency of the EM waves can become lower than the local Langmuir frequency. On the contrary, if the frequency of the plasma is higher than that of laser in the beginning, the incident laser does not need to travel too much before the solitons can be quickly formed. As the density continues to increase above or decrease below the threshold, solitons cease to exist. The threshold of the existence of the solitons is therefore yet to be determined.

As the normalized value a increases, so does the existence range of solitons, which is shown in Fig. 4(a), when the incident laser wavelength is 3 μm. The lower limit of the normalized intensity that can generate visible solitons in simulations is between 0.4 and 0.5, which is not shown in Fig. 4(a). The shaded areas in Fig. 4(b) approximately mark the range of the existence of the EM solitons in the exponential coordinate system. Although the desired incident laser intensity is different for different wavelengths, the parameter windows will be almost the

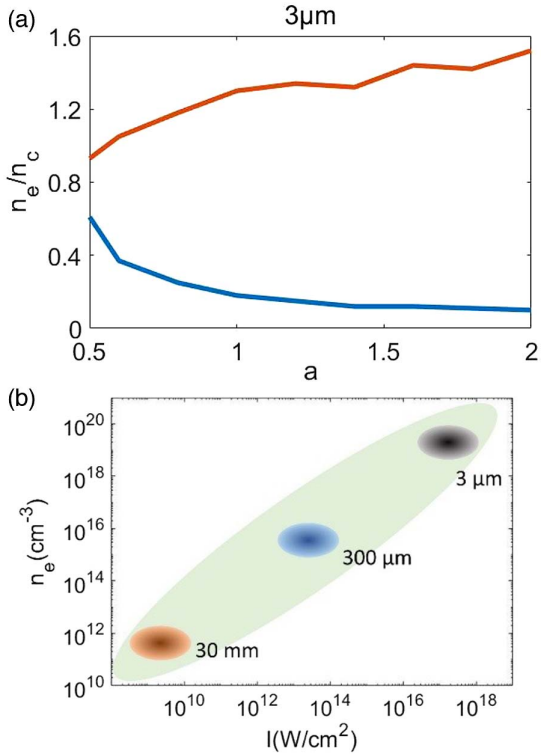

Fig. 4. Panel (a) shows the upper and lower density limits of the existence of solitons at the wavelength of 3 microns. Panel (b) is the existence of solitons at different wavelengths. The abscissa is the intensity of the incident laser, and the ordinate is the density of the plasma. Brown, blue, and black represent the existence criteria of EM solitons when the wavelength of the incident laser is 30 mm, 300 μm, and 3 μm, respectively.

same if the intensity, density, length, and time are in the units of normalized intensity, critical density, laser wavelength, and laser period, respectively, as shown in Fig. 4(a). In other words, the existence of solitons in different wavebands can be predicted according to the assumption that the parameter windows of different wavebands are all the same in the unit of normalized intensity and critical density. For example, for the light of 20 nm, when the corresponding dimensionless amplitude $a = 1$ (that is the intensity of the electric field is $E = 1.61 \times 10^{14}$ V/m and the intensity of incident light is $I = 3.42 \times 10^{21}$ W/cm^2), the range of plasma density for solitons is $0.18 - 1.3n_c$ (that is $5.03 \times 10^{29} - 3.63 \times 10^{30}$ m^{-3}). What we should emphasize is that we are only interested in the formation of solitons in 100 T, and the normalized intensity is around one so that the solitons can be observed obviously while saving computational resources. On the one hand, the formation time over 100 T means extremely low plasma density, where the size of the solitons is many orders of magnitude greater than the laser period. On the other hand, the fact that the higher normalized intensity would lead to the greater plasma density implies that the size of solitons is much smaller than the laser period.

Note the fact that the physical parameters such as length, time, intensity of incident light, and plasma density are all linear with the incident wavelength, which satisfies the invariability

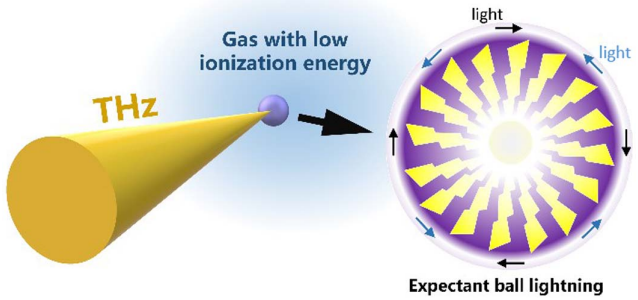

Fig. 5. Composition of the proposed experiment to induce expectant ball lightning EM solitons with high-field THz.

principle of magnification and reduction in the self-similar model. As a result, similar phenomena can be observed regardless of incident wavelength. When the frequency of the incident laser is close to that of the X-ray or even γ-ray level, the size of solitons will get to the nanometer scale, so that the solitons are too small to conduct the observation in the experiment. However, when it comes to the long wavelength, a visible soliton will be formed, theoretically speaking, from our simulation results. Nevertheless, from a practical experimental point of view, the largest microwave-pulse facility currently[19] still cannot reach the energy, which is 10^{10} W/cm^2 at least, to generate expectant ball lightning EM solitons. This requires preionization of the medium to produce plasma with sufficient density, which is difficult to achieve experimentally.

Because of this, we made a proposal to generate expectant ball lightning EM solitons. The proposal is a design of a simulated ball lightning experiment, which uses a strong field THz source as an injected EM wave to interact with the gas and form a gas plasma at the same time, generating an expectant ball lightning EM soliton by controlling the field intensity and the gas plasma density, as seen in Fig. 5. The required THz radiation can be generated by an ultra-intense THz source set up by a femtosecond laser beam, which has been experimentally measured with a 21 MV/m field amplitude at the center frequency of 0.3 THz and a bandwidth of 0.26 THz[26,27]. When the injected EM wave is in the THz band, it can not only meet the requirement of a sufficiently strong THz wave source to ionize the gas to generate gas plasma, but also generate large and observable solitons due to its long wavelength.

3. Conclusion

Ball lightning is a physical phenomenon that many people witness but is extremely difficult to observe with instrument. Although many theories have been analyzed about ball lightning, few of them have the overlapping characteristics about it. Thus, creating a structure like ball lightening in a laboratory is vital for researchers to predict and regenerate ball lightning, and it also provides reference for preventing possible damage caused by ball lightning. In this paper, the dependences of expectant ball lightning EM soliton formation on the wavelength

of the incident light are investigated with two-dimensional PIC simulations. The EM solitons produced by laser–plasma interactions can exist stably for a long time. The electric and magnetic fields can also oscillate constantly at frequencies lower than the localized Langmuir frequency. When the initial density is slightly higher than the critical density, the laser can penetrate a finite length of the plasma and will eventually be trapped to generate solitons due to electron oscillation near the interface. The frequency of the solitons is comparable to that of a laser because photon energy is barely lost. When the initial density is underdense, the laser keeps transferring energy to the plasma until the laser frequency is lower than the localized Langmuir frequency, and the soliton is generated. The difference between the two is whether the laser frequency is higher than the Langmuir frequency. Moreover, the relationship between the soliton position and plasma density is studied, and a more suitable formula has been proposed. The areas where solitons can exist are shown in the shaded figure so that one can figure out the conditions under which solitons can be generated in different wavebands and make appropriate parameters in experiments. In the end, we make a proposal that uses a strong field THz source to inject and interact with gas plasma and produce expectant ball lightning EM solitons, where we observe the resulting phenomena. This proposed experiment has important reference significance for studying ball lightning.

Acknowledgement

This work was supported by the National Natural Science Foundation of China (Nos. 11874372 and 11922412), the Shanghai Rising-Star Program and Shanghai Foundation (No. 2019-jmrh1-kj1), the Strategic Priority Research Program (B) (No. XDB16), the Youth Innovation Promotion Association CAS, and the Key Research Program of Frontier Sciences, CAS (No. ZDBS-LY-SLH018).

References

1. M. Rycroft, "Book review: V. A. Rakov and M. A. Uman, lightning: physics and effects, Cambridge University Press, Cambridge, U.K. 2003, 687 pp. ISBN 0-521-58327-6, 160," Sur. Geophys. **25**, 545 (2004).
2. Y. Liu, T.-J. Wang, N. Chen, G. Hao, H. Sun, L. Zhang, Z. Qi, Z. Wang, and R. Li, "Simultaneous generation of controllable double white light lasers by focusing an intense femtosecond laser pulse in air," Chin. Opt. Lett. **18**, 121402 (2020).
3. D. Zhou, X. Zhang, Q. Lu, Q. Liang, and Y. Liu, "Time-resolved study of the lasing emission from high vibrational levels of N^{2+} pumped with circularly polarized femtosecond pulses," Chin. Opt. Lett. **18**, 023201 (2020).
4. D. Umemoto, H. Tsuchiya, T. Enoto, S. Y. Yamada, T. Yuasa, M. Kawaharada, T. Kitaguchi, K. Nakazawa, M. Kokubun, H. Kato, M. Okano, T. Tamagawa, and K. Makishima, "On-ground detection of an electron-positron annihilation line from thunderclouds," Phys. Rev. E **93**, 021201(R) (2016).
5. M. Shmatov, "Possible detection of high-energy photons from ball lightning," Phys. Rev. E **99**, 043203 (2019).
6. V. Torchigin, "Physical phenomena responsible for stability and spherical form of ball lightning," Optik **219**, 165098 (2020).
7. V. Torchigin and A. V. Torchigin, "Simple explanation of physical nature of ball lightning," Optik **203**, 164013 (2020).
8. M. Shmatov and K. D. Stephan, "Advances in ball lightning research," J. Atmos. Solar-Terrest. Phys. **195**, 105115 (2019).
9. M. L. Shmatov, "New model and estimation of the danger of ball lightning," J. Plasma Phys. **69**, 507 (2003).
10. H. C. Wu, "Relativistic-microwave theory of ball lightning," Sci. Rep. **6**, 28263 (2016).
11. A. Ranada, M. Soler, and J. L. Trueba, "Ball lightning as a force-free magnetic knot," Phys. Rev. E **62**, 7181 (2000).
12. A. Ranada and J. L. Trueba, "Ball lightning an electromagnetic knot?" Nature **383**, 32 (1996).
13. A. I. Egorov and S. I. Stepanov, "Properties of short-living ball lightning produced in the laboratory," Tech. Phys. **53**, 688 (2008).
14. J. A. Menéndez, E. J. Juárez-Pérez, E. Ruisánchez, J. M. Bermúdez, and A. Arenillas, "Ball lightning plasma and plasma arc formation during the microwave heating of carbons," Carbon **49**, 346 (2011).
15. G. D. Shabanov, "On the possibility of making natural ball lightning using a new pulse discharge type in the laboratory," Physics-Uspekhi **62**, 92 (2019).
16. G. Dawson and R. Jones, "Ball lightning as a radiation bubble," Pure Appl. Geophys. **75**, 247 (1969).
17. N. Naumova, S. Bulanov, T. Esirkepov, D. Farina, K. Nishihara, F. Pegoraro, H. Ruhl, and A. Sakharov, "Formation of electromagnetic postsolitons in plasmas," Phys. Rev. Lett. **87**, 185004 (2001).
18. X. Zheng, "Quantitative analysis for ball lightning," Phys. Lett. A **148**, 463 (1990).
19. J. Zhang, D. Zhang, Y. Fan, J. He, X. Ge, X. Zhang, J. Ju, and T. Xun, "Progress in narrowband high-power microwave sources," Phys. Plasmas **27**, 010501 (2020).
20. T. Esirkepov, K. Nishihara, S. V. Bulanov, and F. Pegoraro, "Three-dimensional relativistic electromagnetic subcycle solitons," Phys. Rev. Lett. **89**, 275002 (2002).
21. W. Zhu, J. P. Palastro, and T. M. Antonsen, "Pulsed mid-infrared radiation from spectral broadening in laser wakefield simulations," Phys. Plasmas **20**, 073103 (2013).
22. M. Borghesi, S. Bulanov, D. H. Campbell, R. J. Clarke, T. Z. Esirkepov, M. Galimberti, L. A. Gizzi, A. J. MacKinnon, N. M. Naumova, F. Pegoraro, H. Ruhl, A. Schiavi, and O. Willi, "Macroscopic evidence of soliton formation in multiterawatt laser-plasma interaction," Phys. Rev. Lett. **88**, 135002 (2002).
23. S. V. Bulanov, I. N. Inovenkov, V. I. Kirsanov, N. M. Naumova, and A. S. Sakharov, "Nonlinear depletion of ultrashort and relativistically strong laser-pulses in an underdense plasma," Phys. Fluids B **4**, 1935 (1992).
24. S. V. Bulanov, T. Z. Esirkepov, N. M. Naumova, F. Pegoraro, and V. A. Vshivkov, "Solitonlike electromagnetic waves behind a superintense laser pulse in a plasma," Phys. Rev. Lett. **82**, 3440 (1999).
25. B. Zhu, Y.-C. Wu, K.-G. Dong, W. Hong, J. Teng, W.-M. Zhou, L.-F. Cao, and Y.-Q. Gu, "Observation of a strong correlation between electromagnetic soliton formation and relativistic self-focusing for ultra-short laser pulses propagating through an under-dense plasma," Phys. Plasmas **19**, 102304 (2012).
26. Y. Zeng, Z. Chuliang, L. Song, X. Lu, Z. Li, Y. Ding, Y. Bai, Y. Xu, Y. Tian, J. Liu, R. Li, and Z. Xu, "Guiding and emission of millijoule single-cycle THz pulse from laser driven wire-like targets," Opt. Express **28**, 15258 (2020).
27. S. Feng, L. Dong, T. Wu, Y. Tan, R. Zhang, L. Zhang, C. Zhang, and Y. Zhao, "Terahertz wave emission from water lines," Chin. Opt. Lett. **18**, 023202 (2020).